

# Synthesis and Lithographic Patterning of FePt Nanoparticles Using a Bimetallic Metallopolyyne Precursor\*\*

Kun Liu, Cheuk-Lam Ho, Stephane Aouba, Yi-Qun Zhao, Zheng-Hong Lu, Srebri Petrov, Neil Coombs, Paul Dube, Harry E. Ruda,\* Wai-Yeung Wong,\* and Ian Manners\*

Metal-containing polymers are of intense current interest owing to their combination of unique and intriguing redox, electronic, magnetic, optical, and catalytic properties and their ability to be easily processed and fabricated into thin films, fibers, and other forms.<sup>[1–5]</sup> One of the most promising applications of metal-containing polymers involves their use as precursors for the synthesis of metal nanoparticles (NPs) by thermal or radiation treatment.<sup>[6–12]</sup> As metallopolymers can be readily shaped and patterned using various lithographic techniques, they offer the prospect of access to patterned arrays of metal NPs with control of composition and density per unit area, which are crucial factors for device and catalytic applications.<sup>[11,13,14]</sup> However, many of the most desirable properties are exhibited by metal alloy NPs. To date,

metallopolymer precursors to polymetallic NPs have proven more difficult to synthesize, as they require both the controlled incorporation of different metal atoms into the macromolecular architecture and also appropriate ancillary ligation that does not interfere with the formation of the desired alloy NP product.<sup>[13]</sup>

Iron–platinum alloy NPs have attracted extensive recent attention because of their remarkable magnetic properties.<sup>[15]</sup> In particular, superlattice face-centered tetragonal (fct) FePt NPs exhibit a very large magnetocrystalline anisotropy  $K \approx 5 \times 10^7 \text{ J m}^{-3}$ , one of the highest values among the known hard magnetic materials.<sup>[17]</sup> This large  $K$  value permits a reduction in the size of NPs below 4 nm while retaining the stability of their magnetization against thermal fluctuations and demagnetizing effects.<sup>[18]</sup> These features make the fct FePt NPs highly desirable in the field of ultra-high-density information storage<sup>[19]</sup> and high-performance permanent magnets.<sup>[20]</sup> A general method applied successfully for the synthesis of monodisperse soluble FePt NPs involves a two-step process, that is, high-temperature solution-phase synthesis and thermal annealing.<sup>[21]</sup> Monodisperse FePt NPs can form close-packed NP thin films and superlattices by self-assembly processes.<sup>[15,21,22]</sup> However, a general method to pattern FePt NPs films is not yet available, but such patterning is vital to many device applications, including high-density data storage systems.<sup>[23]</sup> Reports of patterned FePt NP thin films are extremely rare.<sup>[24]</sup> Herein, we report the fabrication of arrays of ferromagnetic FePt NP micro-patterns from thin films of a new air- and moisture-stable, film-forming bimetallic metallopolyyne precursor (**P2**, Scheme 1), which can be utilized directly as a negative resist in both electron-beam lithography (EBL) and UV photolithography.

In searching for appropriate metallized polymer precursors for synthesizing FePt alloy NPs, we chose Pt polyyne that have been extensively studied owing to their unique

[\*] Dr. S. Aouba, Prof. H. E. Ruda  
Centre for Advanced Nanotechnology  
University of Toronto  
Toronto, Ontario, M5S 3E4 (Canada)  
Fax: (+1) 416-978-3801  
E-mail: ruda@ecf.toronto.edu

Dr. C.-L. Ho, Prof. W.-Y. Wong  
Department of Chemistry and  
Centre for Advanced Luminescence Materials  
Hong Kong Baptist University  
Waterloo Road, Kowloon Tong, Hong Kong (China)  
Fax: (+852) 3411-7348  
E-mail: rwywong@hkbu.edu.hk

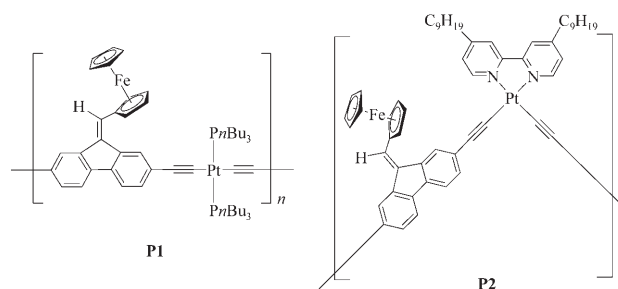
Prof. I. Manners  
The School of Chemistry  
University of Bristol  
Bristol, BS8 1TS (UK)  
Fax: (+44) 117-929-0509  
E-mail: ian.manners@bristol.ac.uk

K. Liu, Dr. S. Petrov, Dr. N. Coombs  
Department of Chemistry  
University of Toronto, Toronto, M5S 3H6 (Canada)  
Y. Zhao, Prof. Z.-H. Lu  
Department of Materials Science and Applied Chemistry  
University of Toronto, Toronto, M5S 3E4 (Canada)

Dr. P. Dube  
Brockhouse Institute for Materials Research  
McMaster University, Hamilton, L8S 4M1 (Canada)

[\*\*] I.M. and H.E.R. are grateful to the NSERC AGENO program for supporting this research, and I.M. thanks the Canadian Government for a Canada Research Chair. W.-Y.W. thanks the Hong Kong Research Grants Council for a CERG grant (project no. HKBU2021/06P) and the Hong Kong Baptist University (FRG/05-06/I-63) for financial support. We also thank Prof. P. D. Harvey for assistance in GPC measurements and H. Wang for DLS measurements.

Supporting information for this article is available on the WWW under <http://www.angewandte.org> or from the author.



Scheme 1. Chemical structures of **P1** and **P2**.

structures and optoelectronic properties.<sup>[25]</sup> We previously reported the synthesis and characterization of the iron-containing polyplatinyne [*trans*-Pt(PnBu<sub>3</sub>)<sub>2</sub>-C≡C-C≡C]<sub>n</sub> **P1** (R = 9-ferrocenylmethylenefluorene-2,7-diyl, Scheme 1), which might be expected to function as a precursor to FePt NPs.<sup>[26]</sup> However, we found that although pyrolysis of **P1** at 700 °C under a N<sub>2</sub> atmosphere yielded fct FePt NPs, as determined by powder X-ray diffraction (PXRD, see the Supporting Information, Figure S1), unwanted phases of Fe<sub>2</sub>P and PtP<sub>2</sub> also existed in the resulting materials. These phosphide materials arise from the presence of the phosphine ligand in the polymer precursor **P1**. It is known that late-transition-metal nitrides are difficult to synthesize because of their low formation enthalpy ( $\Delta H_f$ ).<sup>[27]</sup> To overcome this drawback involving the formation of phosphides, we designed and synthesized a new metallopolyne precursor **P2** (Scheme 1), in which the phosphine ligands were replaced with a bipyridine-type ligand. To our knowledge, this material represents the first example of *cis*-platinum diimine stabilized polyne, although discrete [Pt(diimine)(C≡CAr)<sub>2</sub>] complexes are well-known.<sup>[28]</sup> Polyferroplatinyne **P2** possesses a “kinked” structure with C-Pt-C bond angles of ca. 90° in the metallopolymer main chain and contrasts with the well-known linear rigid-rod metallopolyynes. Metallopolyne **P2** was synthesized by the Cu-catalyzed polycondensation of 9-ferrocenylmethylenefluorene-2,7-diethynylfluorene with dichlorobis(4,4'-dinonyl-2,2'-dipyridyl)platinum in *i*Pr<sub>2</sub>NH/CH<sub>2</sub>Cl<sub>2</sub> at room temperature. The product was isolated as a red powder and was characterized by NMR spectroscopy. The molecular weight was estimated as  $M_w = 11\,900$ ,  $M_n = 8400$ , PDI =  $M_w/M_n = 1.42$  by gel permeation chromatography, and a similar molecular weight was indicated by dynamic light scattering measurements.

We anticipated that a pure FePt phase might be obtained by the pyrolysis of this new polymer precursor **P2**. When polyferroplatinyne **P2** was heated under a N<sub>2</sub> atmosphere at different temperatures (500, 600, and 700 °C) in a tube furnace, black powdery materials were formed, which were attracted to a bar magnet. Figure 1a shows the transmission electron microscopy (TEM) image of the FePt NPs in an amorphous carbonaceous matrix synthesized by pyrolysis of **P2** at 500 °C. Analysis of the TEM image of the NPs indicates that the NPs have an average size of approximately 4 nm and narrow size distribution (standard deviation ca. 10 %, see the Supporting Information, Figure S2).<sup>[29]</sup> The narrow size distribution was obtained by control of the kinetics of NP nucleation and growth,<sup>[30]</sup> which can be achieved by adjusting

the temperature ramp, heating temperature, and duration of heating at certain temperatures. Upon heating **P2** in a tube furnace at a high temperature ramp of 25 °C min<sup>-1</sup> to 500 °C, both Fe and Pt metal atoms are released from the polymer precursor, resulting in the formation of FePt clusters that act as nuclei. The growth proceeds as more Fe and Pt deposit around the nuclei, forming FePt NPs. New nucleation can be hindered by rapidly cooling down the temperature of the tube furnace after it reached 500 °C. Aggregation of the NPs is suppressed by the presence of surrounding carbonaceous matrix. In the control experiments, we found that decreasing the temperature ramp to 2 °C min<sup>-1</sup>, increasing the duration at 500 °C to 2 h, or pyrolysis at higher temperatures (600 and 700 °C) led to larger and polydisperse FePt NPs, as slow nucleation or NP aggregation affects the NP size distribution (see the Supporting Information, Figure S3). Figure 1b shows a high-resolution TEM (HRTEM) image of a single FePt NP with an octahedral shape. The well-faceted shape indicates that the NP is highly crystalline. Lattice fringes are evident, with interfringe distances of 0.38 and 0.27 nm, which are close to the lattice spacing of the (100) planes at 0.385 nm and the (110) planes at 0.272 nm, respectively, in the fct-structured FePt.<sup>[31]</sup> This result revealed that the NP has a single fct FePt alloy phase rather than separate Fe and Pt phases.

The PXRD pattern of the FePt NPs synthesized at 500 °C, as shown in Figure 2, further confirms that the particles have the common chemically ordered fct structure. This result reveals that pyrolysis of **P2** affords a simple one-step reaction to make fct FePt NPs directly, compared to the two-step method of preparing fct FePt NPs involving thermal annealing. The results from Rietveld analysis<sup>[32]</sup> confirmed that the overall long-range order of the synthesized FePt NPs is high, as the microstrain value is almost zero ( $\epsilon_0 = 0.02$ ). These results show that the observed peak broadening should be related mainly to the small sizes of NPs but not to any structural disorder. The mean domain size of approximately 3.6 nm evaluated by Rietveld refinement procedure matches that measured from TEM images, indicating that the as-synthesized fct FePt NPs are composed of nanosized crystalline domains, which form the crystallites in the material. The positions of the diffraction peaks are controlled by the lattice

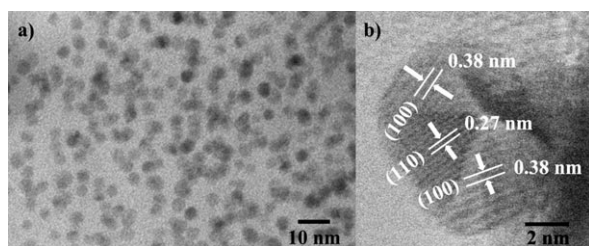


**Figure 1.** TEM bright-field images of a) 4-nm Fe<sub>45</sub>Pt<sub>55</sub> nanoparticles; b) HRTEM of a single FePt nanoparticle with an octahedral shape.

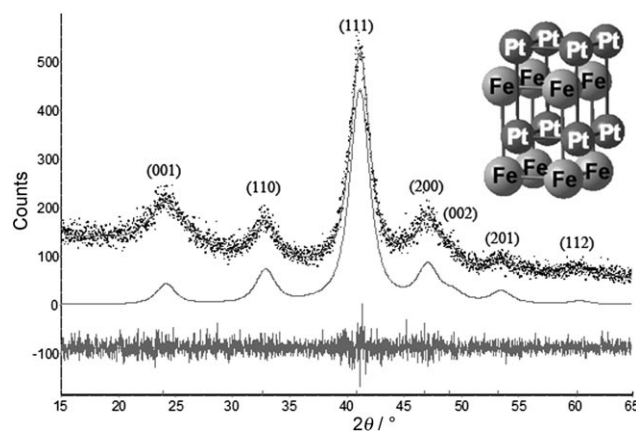


**Figure 2.** Powder X-ray diffraction Rietveld plot of the FePt nanoparticles synthesized at 500 °C under N<sub>2</sub>.

parameters and, therefore, are sensitive to any atomic substitutions within the lattice (solid solutions) that would change their positions on the pattern. Thus, the (111) diffraction peak appears at  $2\theta = 40.82^\circ$ , which is consistent with an Fe content of approximately 46 atom %.<sup>[33]</sup> The FePt NPs appear to be pure, as no  $\text{Fe}_x\text{N}_y$  and  $\text{Pt}_x\text{N}_y$  phases are observed in the PXRD pattern for this sample. As the diffraction pattern only contains peaks from the pure fct FePt phase, the C/N ceramic matrix is essentially amorphous.

The composition of the resulting materials was studied by energy-dispersive X-ray (EDX) elemental analysis. The EDX result (see the Supporting Information, Figure S4) shows the ratio of Fe to Pt to be approximately 0.45:0.55, which is consistent within experimental error with the ratio determined by (111) diffraction-peak position in PXRD. Both ratios are slightly different from the stoichiometry in the polymer precursor (Fe/Pt = 1:1). This small difference can be attributed to the faster loss of potentially volatile Fe-containing fragmentation products compared to the Pt-containing products during pyrolysis.<sup>[13c]</sup>

The zero-field-cooling and field-cooling (ZFC-FC) studies (Figure 3) of temperature-dependent magnetization were performed in a 500-Oe field between 5 and 325 K. The ZFC-FC results reveal that the blocking temperature of the FePt NPs is above 325 K, thus indicating that the FePt NPs are ferromagnetic at room temperature. Superconducting quantum interference device (SQUID) magnetometry measurements show that the 4-nm FePt particles have a relatively high coercivity of 3600 Oe at 5 K and 100 Oe at 300 K. These results confirm that the synthesized FePt NPs have a highly anisotropic fct phase.

In attempts to pattern FePt NPs, a thin film of **P2** (ca. 90 nm) was drop-coated onto a silicon substrate and exposed

to an electron beam. Various electron-beam doses between 2.5 and 25 mCcm<sup>-2</sup> were tested, and a dose of 2.5 mCcm<sup>-2</sup> was optimal among the testing range for obtaining uniformly patterned features and sufficient adhesion to the substrate following development in  $\text{CH}_2\text{Cl}_2$ . Figure 4a shows an optical micrograph of an array of electron-beam fashioned microbars (ca.  $1.0 \times 10 \mu\text{m}^2$ ). Clearly, the unexposed polymer was

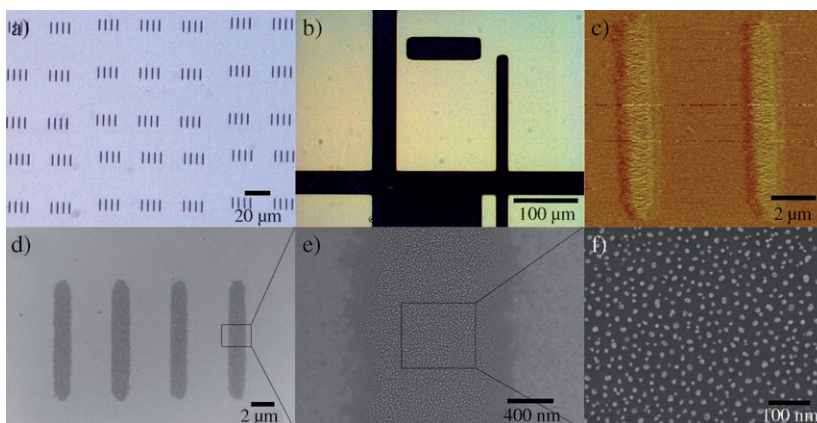


**Figure 4.** Optical micrographs of **P2** a) microbars formed by electron-beam lithography and b) patterns fabricated using UV-photolithography with a chrome contact mask; c) MFM and d–f) SEM images of microbars pyrolyzed at 500°C under  $\text{N}_2$ .

completely removed during development, indicating that **P2** acts as a negative resist in EBL. Pyrolysis of the patterned **P2** microbars at 500°C under a  $\text{N}_2$  atmosphere afforded FePt NP patterns with excellent shape retention (Figure 4d). The SEM images (Figure 4d–f) of the pyrolyzed bars showed that well-faceted NPs densely covered the bars' surfaces with an average size of approximately 9 nm. The magnetic force microscopy (MFM) image of the pyrolyzed bars indicated that they consist of heterogeneous ferromagnetic NPs whose magnetic dipoles appear to be randomly oriented (Figure 4c). The SEM and magnetic data are consistent with the formation of an fct FePt alloy phase as found in bulk experiments. For example, Fe and Pt phases do not phase-separate, because  $\alpha$ -Fe NPs with size of 9 nm would not be ferromagnetic but superparamagnetic.<sup>[34]</sup>

Photolithography is routinely used in the microelectronics industry for parallel patterning over large areas. We found that **P2** can also be utilized as a negative-tone photoresist upon exposure to UV light. After a thin film of **P2** on a silicon substrate was exposed to UV light ( $\lambda = 200\text{--}350 \text{ nm}$ , 80 W) through a chrome contact mask for 60 min, development in  $\text{CH}_2\text{Cl}_2$  gave sharp features (20  $\mu\text{m}$  and above) and completely removed any unexposed polymer (Figure 4b). Lines in the pattern showed excellent shape retention and well-defined edges. We also found that patterns cannot be obtained by treating the film of **P2** with UV light of longer wavelength ( $\lambda > 350 \text{ nm}$ ), even at higher power (450 W) with the same exposure time. In addition, **P1** can also be cross-linked by UV light using a procedure similar to that used for **P2**. The mechanism for the UV photo-cross-linking of **P1** and **P2** is currently under study.

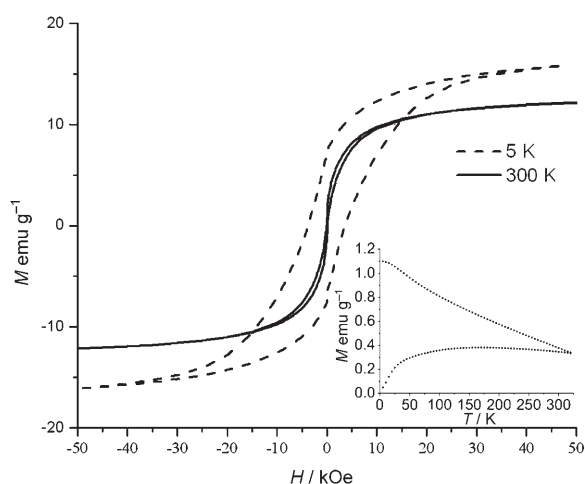


**Figure 3.** Hysteresis loops of the synthesized 4-nm FePt nanoparticles measured at 5 K and 300 K. The zero-field-cooling and field-cooling results are shown in the inset.



In summary, we report herein a novel one-step synthesis of ferromagnetic, fct FePt NPs from a new air- and moisture-stable, readily processed film-forming bimetallic polyferroplatinyne precursor, which can be utilized directly as a negative resist to fabricate array patterns of FePt NPs with high magnetocrystalline anisotropy by both electron-beam lithography<sup>[35]</sup> and UV photolithography. This new approach offers much potential for incorporation into integrated circuit (IC) technology. Future work will focus on the creation of patterned magnetic films for the fabrication of spintronic “switching” devices (e.g. magnetoresistive random access memory (MRAM)),<sup>[36]</sup> nanogranular in gap structures,<sup>[37]</sup> magnetic sensing heads,<sup>[38]</sup> and devices for high-density magnetic data storage<sup>[17,19]</sup> in which the convenient and rapid patterning of magnetic NPs is highly desirable.<sup>[23]</sup>

Received: July 17, 2007

Revised: September 28, 2007

Published online: January 3, 2008

**Keywords:** iron · lithography · materials science · nanostructures · platinum

- [1] R. D. Archer, *Inorganic and Organometallic Polymers*, Wiley, New York, **2001**.
- [2] G. R. Newkome, E. He, C. N. Moorefield, *Chem. Rev.* **1999**, *99*, 1689.
- [3] D. Astruc, F. Chardac, *Chem. Rev.* **2001**, *101*, 2991.
- [4] G. R. Whittell, I. Manners, *Adv. Mater.* **2007**, *19*, 3439.
- [5] See, for example, a) W.-Y. Wong, X.-Z. Wang, Z. He, A. B. Djurišić, C.-T. Yip, K.-Y. Cheung, H. Wang, C. S. K. Mak, W.-K. Chan, *Nat. Mater.* **2007**, *6*, 521; b) A. Arsenault, D. Puzzo, I. Manners, G. A. Ozin, *Nat. Photonics* **2007**, *1*, 468; c) Y. Ma, W.-F. Dong, M. A. Hempenius, H. Möhwald, G. J. Vancso, *Nat. Mater.* **2006**, *5*, 724.
- [6] For work on Fe NPs: a) S. Yajima, M. Omori, *Nature* **1977**, *267*, 823; b) E. J. Houser, T. M. Keller, *Macromolecules* **1998**, *31*, 4038; c) M. J. MacLachlan, M. Ginzburg, N. Coombs, T. W. Coyle, N. P. Raju, J. E. Greedan, G. A. Ozin, I. Manners, *Science* **2000**, *287*, 1460; d) M. J. MacLachlan, M. Ginzburg, N. Coombs, N. P. Raju, J. E. Greedan, G. A. Ozin, I. Manners, *J. Am. Chem. Soc.* **2000**, *122*, 3878; e) M. Ginzburg, M. J. MacLachlan, S. M. Yang, N. Coombs, T. W. Coyle, N. P. Raju, J. E. Greedan, R. H. Herber, G. A. Ozin, I. Manners, *J. Am. Chem. Soc.* **2002**, *124*, 2625; f) C. Park, J. E. McAlvin, C. L. Fraser, E. L. Thomas, *Chem. Mater.* **2002**, *14*, 1225; g) Q. Sun, K. Xu, H. Peng, R. Zheng, M. Häussler, B. Z. Tang, *Macromolecules* **2003**, *36*, 2309.
- [7] For applications of Fe NPs derived from metallopolymer in catalysis: a) S. Lastella, Y. J. Jung, H. Yang, R. Vajtai, P. M. Ajayan, C. Y. Ryu, D. A. Rider, I. Manners, *J. Mater. Chem.* **2004**, *14*, 1791; b) C. Hinderling, Y. Keles, T. Stöckli, H. F. Knapp, T. de Los Arcos, P. Oelhafen, I. Korczagin, M. A. Hempenius, G. J. Vancso, R. Pugin, H. Heinzelmann, *Adv. Mater.* **2004**, *16*, 876; c) J. Q. Lu, T. E. Kopley, N. Moll, D. Roitman, D. Chamberlin, Q. Fu, J. Liu, T. P. Russell, D. A. Rider, I. Manners, M. A. Winnik, *Chem. Mater.* **2005**, *17*, 2227.
- [8] For work on metallopolymer-derived Ru NPs: B. F. G. Johnson, K. M. Sanderson, D. S. Shephard, D. Ozkaya, W. Zhou, H. Ahmed, M. D. R. Thomas, L. Gladden, M. Mantle, *Chem. Commun.* **2000**, 1317.
- [9] For work on metallopolymer-derived Co NPs: a) L. A. Miinea, L. B. Sessions, K. D. Ericson, D. S. Glueck, R. B. Grubbs, *Macromolecules* **2004**, *37*, 8967; b) S. Scholz, P. J. Leech, B. C. Englert, W. Sommer, M. Weck, U. H. F. Bunz, *Adv. Mater.* **2005**, *17*, 1052.
- [10] For work on metallopolymer-derived Ni NPs: L. Friebe, K. Liu, B. Obermeier, S. Petrov, P. Dube, I. Manners, *Chem. Mater.* **2007**, *19*, 2630.
- [11] For work on metallopolymer-derived Au NPs: M. K. Corbierre, J. Beerens, J. Beauvais, R. B. Lennox, *Chem. Mater.* **2006**, *18*, 2628.
- [12] For work on synthesis of metal NPs from small organometallic molecular precursors in polymer matrix: N. Dan, M. Zubris, R. Tannenbaum, *Macromolecules* **2005**, *38*, 9243, and references therein.
- [13] This approach has been successfully used to prepare FeCo NPs from polymetalloocene precursors: a) A. Berenbaum, M. Ginzburg-Margau, N. Coombs, A. J. Lough, A. Safa-Sefat, J. E. Greedan, G. A. Ozin, I. Manners, *Adv. Mater.* **2003**, *15*, 51; b) S. B. Clendenning, S. Aouba, M. S. Rayat, D. Grozea, J. B. Sorge, P. M. Brodersen, R. N. S. Sodhi, Z.-H. Lu, C. M. Yip, M. R. Freeman, H. E. Ruda, I. Manners, *Adv. Mater.* **2004**, *16*, 215; c) K. Liu, S. B. Clendenning, L. Friebe, W. Y. Chan, X. B. Zhu, M. R. Freeman, G. C. Yang, C. M. Yip, D. Grozea, Z.-H. Lu, I. Manners, *Chem. Mater.* **2006**, *18*, 2591.
- [14] a) W. Y. Chan, S. B. Clendenning, A. Berenbaum, A. J. Lough, S. Aouba, H. E. Ruda, I. Manners, *J. Am. Chem. Soc.* **2005**, *127*, 1765; b) C. Díaz, M. L. Valenzuela, *Macromolecules* **2006**, *39*, 103.
- [15] S. Sun, *Adv. Mater.* **2006**, *18*, 393.
- [16] This superlattice face-centered tetragonal fct structure is commonly used in the literature for understanding the crystal structure more easily, since the fct FePt phase normally is transferred from a chemically disordered face-centered cubic fcc FePt phase, in which Fe and Pt atoms are randomly dispersed in the lattice (see reference [15]). Furthermore, in most literature regarding FePt alloy, the “superlattice” was neglected (see references [15, 20, 21]) and only “fct” was used to describe the lattice. FePt alloy actually has a primitive tetragonal structure. Its space group is *P4/mmm* (123), with Strukturbericht designation *L1<sub>0</sub>*.
- [17] D. Weller, M. F. Doerner, *Annu. Rev. Mater. Sci.* **2000**, *30*, 611.
- [18] D. Weller, A. Moser, L. Folks, M. E. Best, W. Lee, M. F. Toney, M. Schwickert, J.-U. Thiele, M. F. Doerner, *IEEE Trans. Magn.* **2000**, *36*, 10.
- [19] a) D. Weller, A. Moser, *IEEE Trans. Magn.* **1999**, *35*, 4423; b) A. Moser, K. Takano, D. T. Margulies, M. Albrecht, Y. Sonobe, Y. Ikeda, S. Sun, E. E. Fullerton, *J. Phys. D* **2002**, *35*, R157.
- [20] a) E. F. Kneller, R. Hawig, *IEEE Trans. Magn.* **1991**, *27*, 3588; b) R. Skomski, J. M. D. Coey, *Phys. Rev. B* **1993**, *48*, 15812; c) T. Schrefl, H. Kronmüller, J. Fidler, *J. Magn. Magn. Mater.* **1993**, *127*, L273; d) H. Zeng, J. Li, J. P. Liu, Z. L. Wang, S. Sun, *Nature* **2002**, *420*, 395.
- [21] S. Sun, C. B. Murray, D. Weller, L. Folks, A. Moser, *Science* **2000**, *287*, 1989.
- [22] For other NPs self-assembled to 1D, 2D, and 3D structures: a) G. A. DeVries, M. Brunnbauer, Y. Hu, A. M. Jackson, B. Long, B. T. Neltner, O. Uzun, B. H. Wunsch, F. Stellacci, *Science* **2007**, *315*, 358; b) A. M. Jackson, J. W. Myerson, F. Stellacci, *Nat. Mater.* **2004**, *3*, 330; c) C. J. Kiely, J. Fink, M. Brust, D. Bethell, D. J. Schiffrin, *Nature* **1998**, *396*, 444; d) C. B. Murray, S. Sun, H. Doyle, T. Betley, *MRS Bull.* **2001**, *26*, 985.
- [23] C. A. Ross, *Annu. Rev. Mater. Sci.* **2001**, *31*, 203.
- [24] a) M. Chen, D. E. Nikles, H. Yin, S. Wang, J. W. Harrell, S. A. Majetich, *J. Magn. Magn. Mater.* **2003**, *266*, 8; b) H. F. Hamann, S. I. Woods, S. Sun, *Nano. Lett.* **2003**, *3*, 1643; c) S. B. Darling, N. A. Yufa, A. L. Cisse, S. D. Bader, S. J. Sibener, *Adv. Mater.* **2005**, *17*, 2446.
- [25] a) W.-Y. Wong, C.-L. Ho, *Coord. Chem. Rev.* **2006**, *250*, 2627; b) W.-Y. Wong, *J. Inorg. Organomet. Polym. Mater.* **2005**, *15*, 197;

- c) N. J. Long, C. K. Williams, *Angew. Chem.* **2003**, *115*, 2690; *Angew. Chem. Int. Ed.* **2003**, *42*, 2586; d) Y. Fujikura, N. Hagihara, K. Sonogashira, *Adv. Chem. Lett.* **1975**, 1067.
- [26] W.-Y. Wong, W.-K. Wong, P. R. Raithby, *J. Chem. Soc. Dalton Trans.* **1998**, 2761.
- [27] S. M. Owen, A. T. Brooker, *A Guide to Modern Inorganic Chemistry*, Wiley, New York, **1991**.
- [28] a) J. E. McGarrah, R. Eisenberg, *Inorg. Chem.* **2003**, *42*, 4355; b) T. J. Wadas, S. Chakraborty, R. J. Lachicotte, Q.-M. Wang, R. Eisenberg, *Inorg. Chem.* **2005**, *44*, 2628; c) S.-C. Chan, M. C. W. Chan, Y. Wang, C.-M. Che, K.-K. Cheung, N. Zhu, *Chem. Eur. J.* **2001**, *7*, 4180; d) C. J. Adams, P. R. Raithby, *J. Organomet. Chem.* **1999**, 578, 178.
- [29] In Figure 1 a, apparent aggregations of the FePt NPs in some areas are actually superpositions of the NPs from different levels in the ceramic matrix.
- [30] C. B. Murray, C. R. Kagan, M. G. Bawendi, *Annu. Rev. Mater. Sci.* **2000**, *30*, 545.
- [31] J. Crangle, J. A. Shaw, *Philos. Mag.* **1962**, *7*, 207.
- [32] G. Will, *Powder Diffraction: The Rietveld Method and the Two Stage Method to Determine and Refine Crystal Structures from Powder Diffraction Data*, Springer, Berlin, **2006**.
- [33] T. J. Klemmer, N. Shukla, C. Liu, X. W. Wu, E. B. Svedberg, O. Mryasov, R. W. Chantrell, D. Weller, M. Tanase, D. E. Laughlin, *Appl. Phys. Lett.* **2002**, *81*, 2220.
- [34] The thermally stable size of  $\alpha$ -Fe NPs is 14 nm. Below this size, the  $\alpha$ -Fe NPs are superparamagnetic. See Reviews on magnetic NPs: D. L. Leslie-Pelecky, R. D. Rieke, *Chem. Mater.* **1996**, *8*, 1770; A.-H. Lu, E. L. Salabas, F. Schüth, *Angew. Chem.* **2007**, *119*, 1242; *Angew. Chem. Int. Ed.* **2007**, *46*, 1222.
- [35] Although in the proof-of-concept experiments described herein we pattern on the micrometer scale, EBL is capable of resolutions down to 10–50 nm. See J. R. Sheats, B. W. Smith, *Microolithography*, Marcel Dekker, New York **1998**.
- [36] S. A. Wolf, D. D. Awschalom, R. A. Buhrman, J. M. Daughton, S. von Molnár, M. L. Roukes, A. Y. Chtchelkanova, D. M. Treger, *Science* **2001**, *294*, 1488.
- [37] M. B. A. Jalil, *IEEE Trans. Magn.* **2002**, *38*, 2613.
- [38] R. E. Fontana, J. Katine, M. Rooks, R. Viswanathan, J. Lille, S. MacDonald, E. Kratschmer, C. Tsang, S. Nguyen, N. Robertson, P. Kasiraj, *IEEE Trans. Magn.* **2002**, *38*, 95.